

# Novel Peptides Derived from Dengue Virus Capsid Protein Translocate Reversibly the Blood–Brain Barrier through a Receptor-Free Mechanism

Vera Neves,<sup>†</sup> Frederico Aires-da-Silva,<sup>‡</sup> Maurício Morais,<sup>§</sup> Lurdes Gano,<sup>§</sup> Elisabete Ribeiro,<sup>§</sup> Antónia Pinto,<sup>†</sup> Sandra Aguiar,<sup>‡</sup> Diana Gaspar,<sup>†</sup> Célia Fernandes,<sup>§</sup> João D. G. Correia,<sup>§</sup> and Miguel A. R. B. Castanho<sup>\*,†</sup>

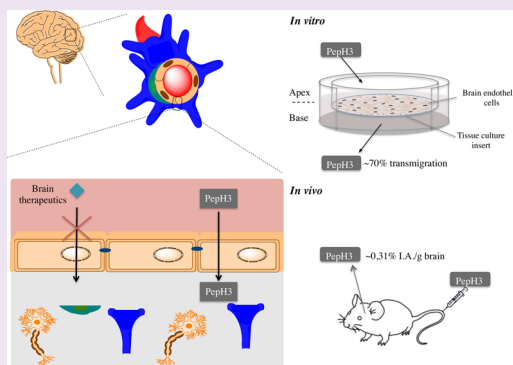
<sup>†</sup>Instituto de Medicina Molecular, Faculdade de Medicina, Universidade de Lisboa, Av. Prof. Egas Moniz, 1649-028 Lisboa, Portugal

<sup>‡</sup>CIISA - Faculdade de Medicina Veterinária, Universidade de Lisboa, Avenida da Universidade Técnica, 1300-477 Lisboa, Portugal

<sup>§</sup>Centro de Ciências e Tecnologias Nucleares, Instituto Superior Técnico, Universidade de Lisboa, Campus Tecnológico e Nuclear, Estrada Nacional 10 (km 139,7), 2695-066 Bobadela LRS, Portugal

## Supporting Information

**ABSTRACT:** The delivery of therapeutic molecules to the central nervous system is hampered by poor delivery across the blood–brain barrier (BBB). Several strategies have been proposed to enhance transport into the brain, including invasive techniques and receptor-mediated transport (RMT). Both approaches have several drawbacks, such as BBB disruption, receptor saturation, and off-target effects, raising safety issues. Herein, we show that specific domains of Dengue virus type 2 capsid protein (DEN2C) can be used as trans-BBB peptide vectors. Their mechanism of translocation is receptor-independent and consistent with adsorptive-mediated transport (AMT). One peptide in particular, named PepH3, reaches equilibrium distribution concentrations across the BBB in less than 24 h in a cellular *in vitro* assay. Importantly, *in vivo* biodistribution data with radiolabeled peptide derivatives show high brain penetration. In addition, there is fast clearance from the brain and high levels of excretion, showing that PepH3 is a very good candidate to be used as a peptide shuttle taking cargo in and out of the brain.



Due to aging and other societal factors, the prevalence of neurological disorders is growing and is presently a public health priority and an important cause of mortality: 12% of total deaths worldwide.<sup>1</sup> Despite rapid developments in understanding brain function and the great advances in medical technology, many central nervous system (CNS)-associated malignancies remain devastating and poorly treated.<sup>2</sup> The reasons for the low success rates of CNS-targeted treatments are mainly related to incomplete understanding of the brain biochemistry and physiology, the high susceptibility for side effects, shortage of validated biomarkers for assessing therapeutic efficacy, and poor delivery to the brain. The main hurdle for effective CNS drug delivery is the blood–brain barrier (BBB), formed by brain endothelial cells richly connected by tight junctions that selectively limit the transfer of substances between the blood and the interstitial fluid of the CNS and *vice versa*.<sup>3</sup> It is estimated that approximately 98% of small molecules and nearly all large molecules, such as recombinant proteins or gene-based medicines,<sup>4</sup> are unable to cross the BBB. BBB disruption or transient opening<sup>5</sup> is a possibility to overcome this limitation, but these invasive strategies remain technically challenging and raise safety concerns.<sup>6</sup> Hence, effective and safe alternative approaches

should be carefully designed to avoid compromising the overall protective function of BBB.<sup>7</sup>

Compounds that are able to traverse the BBB may use active or passive mechanisms. Small lipophilic molecules tend to enter the brain by passive diffusion. Nutrients such as glucose and amino acids use specific carriers present on endothelial membranes to be transported to the brain. In contrast, larger molecules (*e.g.*, peptides and proteins) able to transverse the BBB are transported either *via* receptor-mediated transcytosis (RMT) or adsorptive-mediated transcytosis (AMT). Peptides, modified proteins, or monoclonal antibodies may explore both entry routes.<sup>8</sup> RMT pathways carry macromolecules such as insulin, leptin, and transferrin into the brain.<sup>9</sup> Engineered ligands that explore RMT are known as “molecular Trojan horses,” which can bind BBB receptors and deliver therapeutic molecules across the BBB.<sup>10–12</sup> The efficiency of transport across the BBB, however, is limited by the number of receptors exposed in brain endothelial cells (BECs) and poor penetration

**Received:** February 2, 2017

**Accepted:** March 6, 2017

**Published:** March 6, 2017

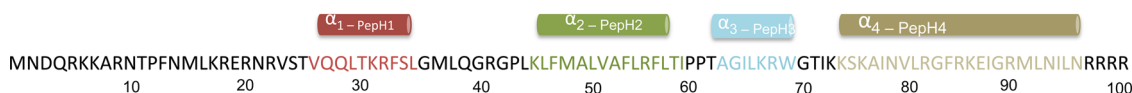


**Figure 1.** Dengue virus capsid protein (DEN2C) sequence. DEN2C is a 12 kDa protein, with 100 amino acid residues. The protein is formed by four helical domains,  $\alpha_1$ ,  $\alpha_2$ ,  $\alpha_3$ , and  $\alpha_4$ , designated PepH1, PepH2, PepH3, and PepH4, respectively.

of drugs into the brain.<sup>9</sup> The transferrin and the insulin receptors (TfR and IR, respectively) are examples of well-studied receptors for brain targeting that, however, are highly and broadly expressed in other tissues and are also implicated in crucial cellular functions, creating safety risks.<sup>13,14</sup> Over past years, there has been an effort to identify new BBB RMT targets that have better BBB specificity. For example, the heavily glycosylated protein Cdc50A, recognized by the FCS single domain antibody selected by functional panning of the llama VHH phage-display library, is internalized into BECs.<sup>15</sup> Biodistribution assays reveal high brain uptake: 2.9% injected dose per gram of tissue (ID/g of tissue).<sup>16</sup> Recent work from Zuchero *et al.* reveals other adequate receptors for BBB-specific RMT, such as basigin, Glut1, and CD98hc, the latter enabling considerable accumulation in the brain (0.4% ID/g of tissue) of radiolabeled antibodies.<sup>17</sup> In addition, by using bispecific antibodies that bind to CD98hc on one arm, and the amyloid precursor protein (APP) cleavage protein enzyme  $\beta$ -secretase (BACE1) on the other arm, it was possible to translocate the BBB and reduce  $A\beta$  production.<sup>17</sup> This method is, however, complex and critically dependent on very few and specific receptors. Besides, there is still a lack of information on the expression of these receptors in other tissues and the general safety profile.

New approaches that overcome the limitations of RMT are urgently needed. AMT is a suitable alternative. AMT is mainly triggered by electrostatic interaction of cationic proteins or peptides with endothelial cells.<sup>18,19</sup> Peptide vectors for AMT are typically cationic due to the presence of lysine and arginine residues in their composition. They can also combine polar and nonpolar/hydrophobic amino acid residues to form amphipathic domains that facilitate cellular uptake. Several examples of receptor-independent peptide vectors include the transactivating transcriptional activator (TAT) from the human immunodeficiency virus 1 (HIV-1), the third helix of the Antennapedia homeodomain (Antp), and SynB1 derived from protegrins, among others.<sup>20,21</sup> These peptides deliver different cargos across a variety of endothelial cells, including BECs.<sup>22</sup> For instance, SynB1 and D-penetratin were used to deliver doxorubicin to the brain, using *in situ* rat brain perfusion.<sup>23</sup> Furthermore, TAT was fused to  $\beta$ -galactosidase ( $\beta$ -gal) and administered to mice.  $\beta$ -gal activity in the brain was detected without affecting the integrity of the BBB.<sup>24</sup> A recent study has also shown the uptake of angioprep-2 paclitaxel conjugate into the brain with improved delivery to the brain and brain metastases of breast cancer compared to free paclitaxel.<sup>25</sup>

Although the proof of concept has been validated for more than 15 years,<sup>24</sup> the quest for efficient cost-effective trans-BBB receptor-independent peptide vectors remains. Recently, we have shown that viral proteins are an underexplored source of peptide vector templates,<sup>26</sup> as viruses have the ability to penetrate cells very efficiently. Some short sequences of the Dengue virus type-2 capsid protein (DEN2C) are particularly efficient in cellular membrane translocation, one of them using receptor-independent routes.<sup>27,28</sup> DEN2C is a highly basic protein with the capacity to translocate cell membranes

carrying macromolecules,<sup>28,29</sup> which prompted us to carry out a systematic study of the helical domains of this protein as trans-BBB vectors. Translocation of the BBB by DEN2C derived peptides was tested both *in vitro* and *in vivo*. One domain, PepH3, achieved promising brain penetration as demonstrated by *in vitro* and *in vivo* studies.

## RESULTS

**Selection of Peptide Sequences.** The viral genome of Dengue virus (DENV) consists of a single-stranded, positive sense RNA molecule that is complexed to multiple copies of the capsid protein (DEN2C). The nucleocapsid is surrounded by a host-derived lipid membrane, in which two transmembrane proteins are inserted, the major envelop glycoprotein E and the membrane protein M.<sup>30</sup> DEN2C protein is highly charged, and its structure, determined by NMR, comprises four  $\alpha$ -helical domains,  $\alpha_1$ ,  $\alpha_2$ ,  $\alpha_3$ , and  $\alpha_4$  (Figure 1).<sup>27</sup> The protein forms a dimer in which the positive charges on the exposed regions of  $\alpha_4$  have been assigned to have a role in electrostatic RNA binding, while the relatively hydrophobic  $\alpha_2$  regions have been assigned to be putatively responsible for lipid membrane association, but this hypothesis has been challenged.<sup>27</sup> The whole protein and two distinct sequences of amino acids of the protein, PepM ( $\alpha_2$ – $\alpha_3$ ) and PepR ( $\alpha_4$  and C-terminal region rich in arginine residues), have the capacity to deliver nucleic acids into cells.<sup>29</sup> Herein, the isolated helical short domains  $\alpha_1$ ,  $\alpha_2$ ,  $\alpha_3$ , and  $\alpha_4$  (PepH1, PepH2, PepH3, and PepH4, respectively) were studied as trans-BBB peptide vectors. The peptides and their labeled radioactive analogs were synthesized and tested in *in vitro* brain endothelial barrier (BEB) models for translocation efficacy, followed by examination of brain penetration *in vivo* in CD1 mice.

**Synthesis and Characterization of Radiopeptides.** First, PepH1 to PepH4 were prepared in an automated MW-assisted solid phase peptide synthesizer using the Fmoc strategy. The amino acid sequences, isoelectric point (PI), charge, and mass, determined by electrospray ionization–mass spectrometry (ESI-MS), for all peptides are displayed in Table 1.

The peptide conjugates containing the pyrazol-diamine (Pz) (Pz<sup>1</sup>PepH1, Pz<sup>1</sup>PepH2, Pz<sup>1</sup>PepH3, and Pz<sup>2</sup>PepH4) and the NODA-GA (NODAPepH1 to NODAPepH4) chelating units (Table 1) were prepared by conjugation of the carboxylic acid of the respective bifunctional chelator (Pz<sup>1</sup>, Pz<sup>2</sup> or NODA-GA) to the N-terminal of the peptides (PepH1 to PepH4) on the resin, as described in the Methods section. Following cleavage from the solid support and precipitation with ice-cold diethyl ether, the crude peptide conjugates were purified by semi-preparative RP-HPLC (>95% purity). After lyophilization, the pure peptide conjugates, obtained as white solids, were characterized by ESI-MS. Reaction of the peptide conjugates with the precursor *fac*-[<sup>99m</sup>Tc(CO)<sub>3</sub>(H<sub>2</sub>O)<sub>3</sub>]<sup>+</sup> gave the corresponding radiolabeled peptides TcPz<sup>1</sup>PepH1, TcPz<sup>1</sup>PepH2, TcPz<sup>1</sup>PepH3, and TcPz<sup>2</sup>PepH4 in high radiochemical yield and purity (>90%; Table 1).

Table 1. (Radio)peptide Properties<sup>a</sup>

peptide	sequence	IP	charge	calcd exact mass (Da)	found [ion]	peptide conjugates	calcd exact mass (Da)	found [ion]	$t_R$ (min) peptide conjugates	$t_R$ (min) radiopeptides	$\log P_{o/w}$ of radiopeptides
PepH1	VQQLTKRFSL	11.0	2	1219.4	1220.4 [M + H] <sup>+</sup>	Pz <sup>1</sup> PepH1	1527.8	1527.10 [M + H] <sup>+</sup>	12.1 <sup>b</sup>	TcPz <sup>1</sup> PepH1:16.1 <sup>b</sup>	-1.76 ± 0.11
PepH2	KLFMALVAFLRFLT	11.0	2	1670.1	1671.1 [M + H] <sup>+</sup>	NODAPepH1 Pz <sup>1</sup> PepH2	1576.6 1978.4	789.10 [M + 2H] <sup>2+</sup> 1978.30 [M + H] <sup>+</sup>	13.6 <sup>c</sup> 20.2 <sup>b</sup>	GaNODAPepH1:13.8 <sup>c</sup> TcPz <sup>1</sup> PepH2:22.4 <sup>b</sup>	-2.16 ± 0.04 0.65 ± 0.13
PepH3	AGILKRW	11.0	2	843.0	844.0 [M + H] <sup>+</sup>	NODAPepH2 Pz <sup>1</sup> PepH3	2027.2 1151.3	2027.80 [M + H] <sup>+</sup> 1151.80 [M + H] <sup>+</sup>	23.5 <sup>c</sup> 13.5 <sup>b</sup>	GaNODAPepH2:23.7 <sup>c</sup> TcPz <sup>1</sup> PepH3:15.9 <sup>b</sup>	0.35 ± 0.14 0.11 ± 0.06
PepH4	KSKAINVLGRFKEIGRMLNILN	11.7	6	2671.2	1336.0 [M + 2H] <sup>2+</sup>	NODAPepH3 Pz <sup>2</sup> PepH4	1200.2 2934.5	1200.00 [M + H] <sup>+</sup> 735.40 [M + H] <sup>+</sup>	13.4 <sup>c</sup> 10.6 <sup>b</sup>	GaNODAPepH3:13.7 <sup>c</sup> TcPz <sup>2</sup> PepH4:12.8 <sup>b</sup>	1.21 ± 0.09 -1.84 ± 0.31
						NODAPepH4	3027.4	1010.14 [M + 3H] <sup>3+</sup>	18.2 <sup>c</sup>	GaNODAPepH4:18.4 <sup>c</sup>	-0.80 ± 0.13

<sup>a</sup>Peptide sequences, isoelectric point (IP), charge, molecular weight (MW), HPLC retention time, and octanol–water partition coefficients for all peptide derivatives. <sup>b</sup>Gradient D. <sup>c</sup>Gradient E.

The <sup>67</sup>Ga-labeled peptide conjugates (GaNODAPepH1 to GaNODAPepH4) were prepared in high radiochemical yield and purity (>95%) by reaction of the respective peptide conjugate with the precursor <sup>67</sup>GaCl<sub>3</sub> at RT for 5 min (Table 1).

The octanol–water partition coefficients,  $P_{o/w}$ , were determined for all radioactive peptide conjugates by the “shake flask” method (Table 1) to assess hydrophobicity.<sup>31</sup> The results show that radiolabeled PepH2 and PepH3 are the most hydrophobic. In addition, experiments using lipid membrane models (Supplementary Figure S1 and S2) containing phosphatidylcholine (PC), phosphatidylglycerol (PG), phosphatidylserine (PS), and cholesterol (Chol) show that PepH2 interacts to a greater extent with the zwitterionic POPC and POPC:Chol bilayers followed by the anionic POPC:POPS and POPC:POPG bilayers. It has been proposed that cholesterol plays an important role in facilitating efficient cell entry of DENV and that infectivity can be significantly impaired in cholesterol-depleted cells.<sup>32</sup> PepH3 has a strong preference for anionic POPC:POPS (1:4) bilayers, presenting a lipid bilayer–water partition coefficient ( $K_p$ ) of  $(1.6 \pm 0.2) \times 10^2$ . In addition, both PepH2 and PepH3 present an  $\alpha$ -helical conformation in the presence of LUVs (Figure S2).

**Integrity of the BEB Model.** The *in vitro* BEB model was prepared using brain endothelial cells (bEnd.3) growing in tissue culture inserts (Figure 2A). bEnd.3 is an immortalized mouse brain endothelial cell line with barrier properties, which are widely used as a model for the BBB due to their rapid growth, the maintenance of their properties over repeated passages, and amenability to numerous molecular interventions.<sup>33,34</sup> The integrity of the endothelial barrier was evaluated through the permeability of 5(6)-carboxyfluorescein (FITC) and fluorescently labeled dextrans (FD) with different molecular weights (FITC, 376.32 Da; FD4, 4 kDa; and FD40, 40 kDa; Figure 2B, C, and D, respectively). The clearance of the fluorescent probes from the apical side in the presence or absence of the unlabeled peptides (1  $\mu$ M) was negligible, which demonstrates the lack of both fenestration in the cell barrier and paracellular leakage. Small molecules such as FITC have a residual crossing of the cellular model of the BEB, but molecules with higher molecular weight, such as FD4 or FD40, have negligible translocation. In addition, cell viability assays show that the fraction of viable bEnd.3 cells was above 90%, even at 100  $\mu$ M peptide concentration (Supporting Information Figure S3).

**Translocation across the BEB.** To study the kinetics of the radiopeptides transmigrating through the *in vitro* BEB model, 5  $\mu$ Ci mL<sup>-1</sup> of radiopeptide (TcPz<sup>x</sup>PepH1 to TcPz<sup>x</sup>PepH4, x = 1 or 2) were added to the apical chamber. The apical side (apex) volume, transwell filter covered with cells, and base volume were collected after 15 min and 5 and 24 h (Figure 3A–D), and the radioactivity in those samples measured separately in a  $\gamma$ -counter. Complementary experiments were performed to determine the fraction of peptides associated with the bEnd.3 cell membrane and intracellular space (Figure 4A–D). In this case, cells growing in 24-well plates were incubated with the radiopeptides, washed with an acid buffer to assess the interaction with cell membrane, and finally cells were lysed to determine the cellular internalization. The radioactivity associated with each fraction was then measured in the  $\gamma$ -counter.

The data obtained demonstrated that PepH1 was able to transmigrate the BEB, with up to  $73.8 \pm 9.4\%$  of the peptide

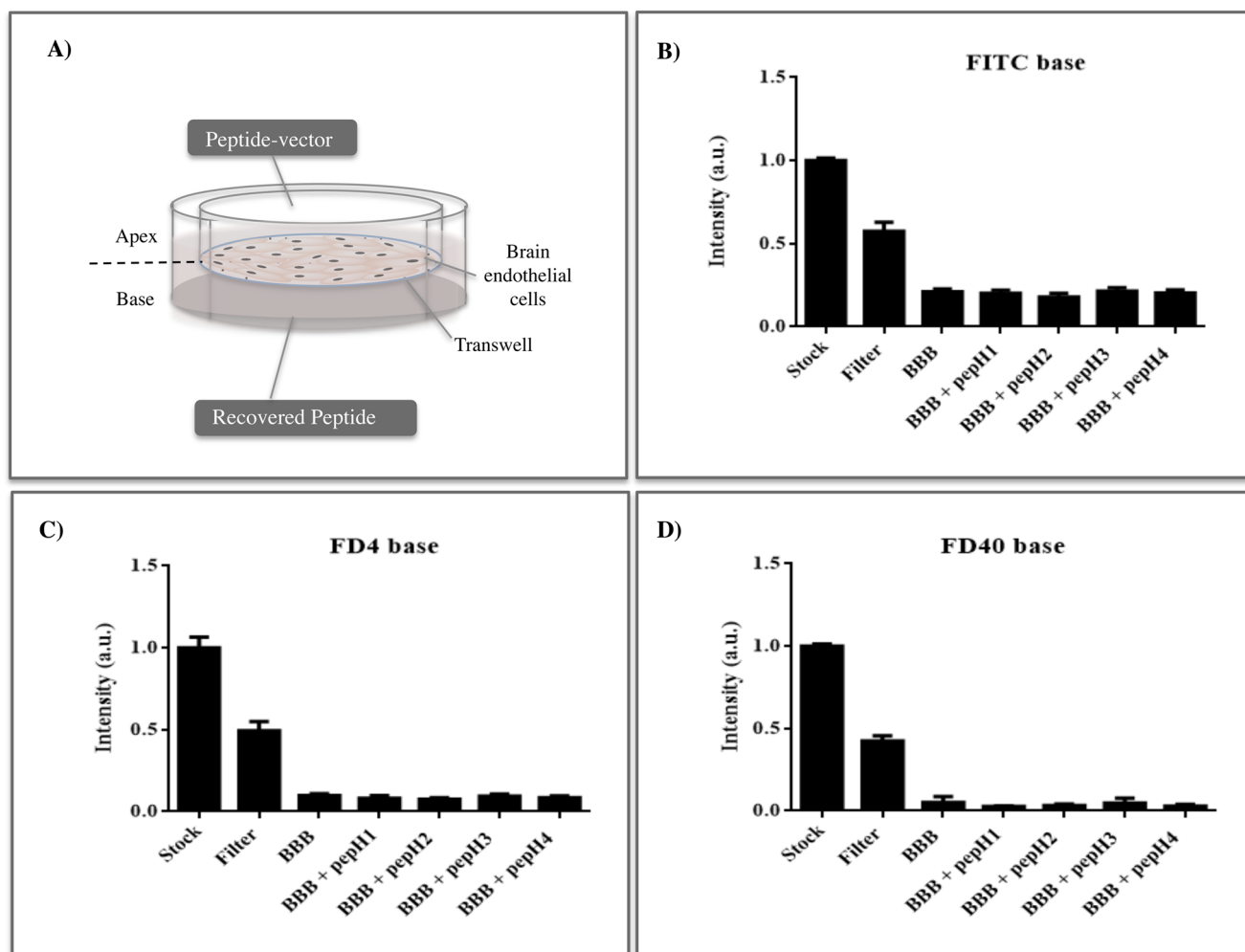


**Figure 2.** Determination of BEB integrity in the presence of peptides. The *in vitro* BEB model consists of a transwell system with an insert in which bEnd.3 cells are grown separating two chambers (A). The insert, or apical side, corresponds to the blood side, while the base (bottom chamber) corresponds to the brain side. Unlabeled peptides ( $1 \mu\text{M}$ ) were added to the top compartment. After 24 h of peptide addition, the fluorescence emission intensity of probes having different molecular weights (FITC with 376.32 Da, FD4 with 4 kDa, and FD40 with 40 kDa) was registered from the base compartment and compared to two controls: one with the naked transwell filter (marked “Filter”) and the other consisting of the fluorescence intensity of the stock solution after stirred dilution (marked “Stock”). Represented values were obtained from triplicates of two independent experiments.

radioactivity found in the base after 24 h (Figure 3A). In addition, PepH1 had minimal internalization and membrane retention ( $0.12 \pm 0.00$  and  $0.38 \pm 0.10\%$ , respectively; Figure 4A). BEB translocation of PepH2 was reduced ( $9.2 \pm 2.5\%$  after 24 h), although it presented high cellular internalization ( $42.7 \pm 0.0\%$  after 24 h; Figures 3B and 4B). Similar to PepH1, BEB translocation of PepH3 was high ( $67.2 \pm 1.2\%$  at 24 h), and the radioactivity associated with the cell (membrane and internalized peptide) was low (Figures 3C and 4C). In contrast to all other peptides, PepH4 had moderate membrane retention, low internalization ( $10.2 \pm 0.8$  and  $2.8 \pm 0.2\%$ , respectively; Figure 3D) and high BEB translocation ( $63.4 \pm 1.9\%$  after 24 h; Figure 4D). It is worth highlighting that the volume of the base is 2.5-fold the volume of the apex. The amount of PepH1, PepH2, PepH3, and PepH4 is also 2.5-fold in the base relative to the volume of the apex, which shows that there is an equilibrium in the distribution of the peptides across the BEB cells, consistent with AMT.

In order to better assess the action of the peptide itself, independent from the radioactive label used, we carried out

similar experiments with  $^{67}\text{Ga}$ -labeled peptides (Table S1). Table 2 compares the results obtained with the two different radioisotopes after 24 h of incubation time, revealing very similar results for BEB translocation. Nevertheless, there are differences in the percentage of internalization and percentage of cellular adsorption for PepH2 and PepH4. The radiometal core influences the retention of peptides by cells. It is noteworthy that the net charge of the final radiopeptide is affected by the radiometal core. Indeed, in the case of  $^{99\text{m}}\text{Tc}$ , the radioactive metal core ( $\text{fac-}[^{99\text{m}}\text{Tc}(\text{CO})_3]^+$ ) is stabilized by a neutral pyrazolyl-diamine chelating unit ( $\text{Pz}^x$ ) giving monocationic radiometal complexes,<sup>35</sup> whereas in the case of  $^{67}\text{Ga}$ , the trivalent metal is stabilized by a trianionic macrocyclic chelator (NODA-GA), which results in neutral radiometal complexes.<sup>36</sup>

**Biodistribution Studies.** The radiopeptides  $\text{TcPz}^1\text{PepH1}$  and  $\text{TcPz}^1\text{PepH3}$  were the molecules with the most promising behavior in the *in vitro* experiments and were therefore selected for evaluation *in vivo*. They were administrated intravenously in CD1 mice and their biodistribution evaluated at two different

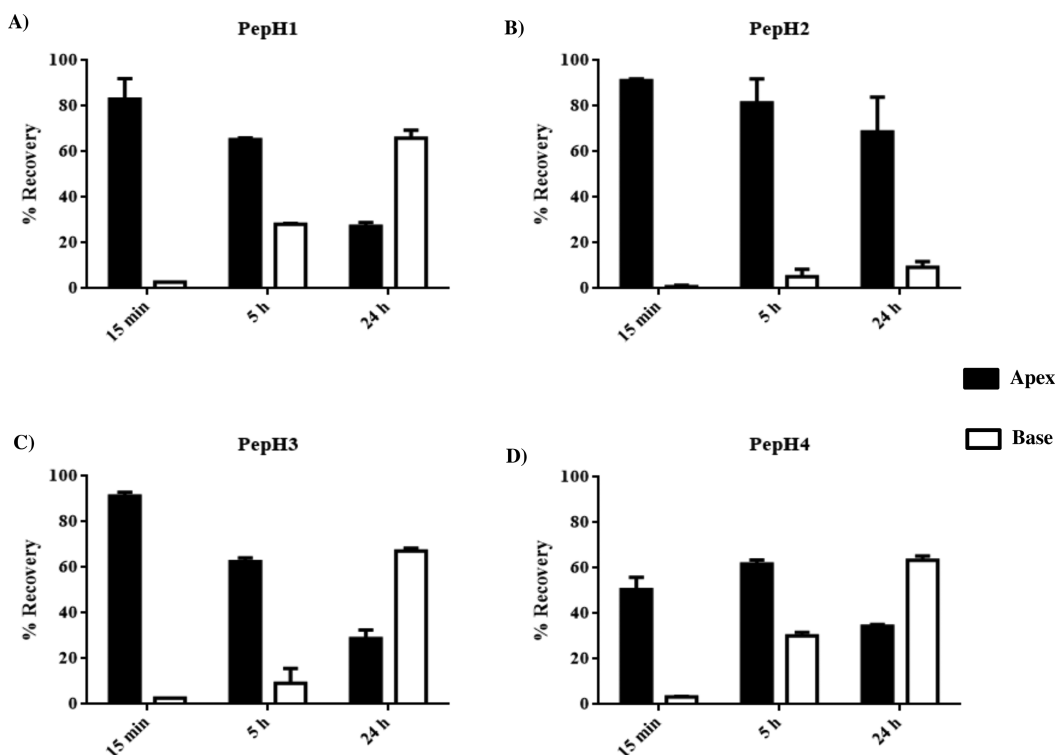


**Figure 3.** Kinetics of translocation of the transwell *in vitro* model of the BBB. A total of  $5 \mu\text{Ci mL}^{-1}$  of radiopeptides ( $\text{TcPz}^x\text{PepH1}$  to  $\text{TcPz}^x\text{PepH4}$ ,  $x = 1$  or  $2$ ) was initially added to the apical side. After 15 min and 5 and 24 h of incubation, the relative amounts of PepH1 (A), PepH2 (B), PepH3 (C), and PepH4 (D) in the apical side plus filter with cells (black bars) and base (white bars) were quantified. The amount in the apex and base was normalized to the initial total amount of labeled peptide added to the top and expressed as the percentage of recovered radioactive dose. PepH1, PepH3, and PepH4 are efficient in BBB translocation, whereas PepH2 has limited passage through the BBB. Values obtained from triplicates of two independent experiments.

time points (5 min and 1 h). As a negative control, the biodistribution profile of  $\text{TcPz}^3$  was also evaluated in the same animal model to demonstrate the low ability of the radiometal core ( $[\text{}^{99\text{m}}\text{Tc}(\text{CO})_3]^+$  stabilized by a model pyrazolyl-diamine containing chelator) to cross the BBB. The pharmacokinetic profile of the radiolabeled peptides was also compared with that of  $^{99\text{m}}\text{Tc}(\text{CO})_3$ -recombinant small domain antibody FC5 that has been previously demonstrated to efficiently penetrate the BBB using RMT.<sup>16</sup> The biodistribution of  $\text{TcPz}^3$ ,  $\text{TcPz}^1\text{PepH1}$ ,  $\text{TcPz}^1\text{PepH3}$ , and  $\text{TcFC5}$  is shown in Table 3. The brain uptake of  $\text{TcPz}^1\text{PepH1}$  and  $\text{TcPz}^1\text{PepH3}$  peptides occurs rapidly after injection ( $>0.1\%$  injected dose per gram of brain after 5 min). Importantly, the data obtained clearly demonstrate that the brain uptake for  $\text{TcPz}^1\text{PepH1}$  ( $0.14 \pm 0.03\%$  ID/g) and  $\text{TcPz}^1\text{PepH3}$  ( $0.31 \pm 0.07\%$  ID/g) at 5 min is, respectively, 1.6- and 3.4-fold higher than the brain accumulation of  $\text{TcPz}^3$  ( $0.09 \pm 0.01\%$  ID/g). These results clearly show that the biological BBB crossing activity of PepH1 and PepH3 can be assigned to the peptide sequence and not to the radiometal core. Moreover, both peptides have rapid brain washout (down to  $<0.03 \pm 0.01\%$  ID/g after 1 h), concomitant with fast elimination of the total radioactivity from most organs: radiopeptides were rapidly cleared from blood, liver, kidney, and highly irrigated organs, accumulating in the intestine ( $>10\%$ ). Indeed, an important fraction of the activity was excreted ( $>30\%$ ) 1 h after injection (Table 3). In addition, when we compare the pharmacokinetic profiles of  $\text{TcPz}^1\text{PepH1}$  and  $\text{TcPz}^1\text{PepH3}$  peptides with the biodistribution profile of  $\text{TcFC5}$ , we can see that PepH3 showed a similar BBB crossing at 5 min post injection ( $0.47 \pm 0.27\%$  ID/g). Furthermore,  $\text{TcPz}^1\text{PepH3}$  is rapidly excreted at

higher percentages ( $36.0 \pm 11.2\%$  ID/g) when compared with  $\text{TcFC5}$  ( $9.6 \pm 1.4\%$  ID/g), which is extremely positive to avoid toxic effects associated with accumulation in the brain and other organs. Brought together, the *in vivo* results show that although  $\text{TcPz}^1\text{PepH1}$  displays a more modest brain accumulation,  $\text{TcPz}^1\text{PepH3}$  exhibited a robust brain uptake and can be a good candidate as a shuttle peptide for taking cargo in and out of the brain.

**Chemical Stability in Blood and Urine.** The analysis of tissue samples collected from the sacrificed mice at 5 min and 1 h showed that radiopeptides are relatively stable in the blood, but in urine they are partially degraded with new radiochemical species appearing at lower retention times after 1 h. Figure 5 shows the RP-HPLC chromatograms of the radiolabeled peptides PepH1 and PepH3 before administration and in mice blood serum and urine collected 5 min and 1 h after administration.

## DISCUSSION

The capsid protein of Dengue virus type 2 (DEN2C) is able to translocate cell membranes carrying proteins and genes that remain functional in the intracellular space.<sup>28,29</sup> This property has led to the hypothesis that capsid protein intervenes in the viral penetration of cells.<sup>37,38</sup> Two distinct peptides, corresponding to two separate domains of DEN2C, retain the cell-penetrating properties of the parent protein.<sup>29</sup> Here, we performed a systematic study of the four highly structured helical domains of DEN2C, having the sequences PepH1, PepH2, PepH3, and PepH4 peptides (Figure 1 and Table 1), aiming at (i) finding their efficacy in translocating the BBB and

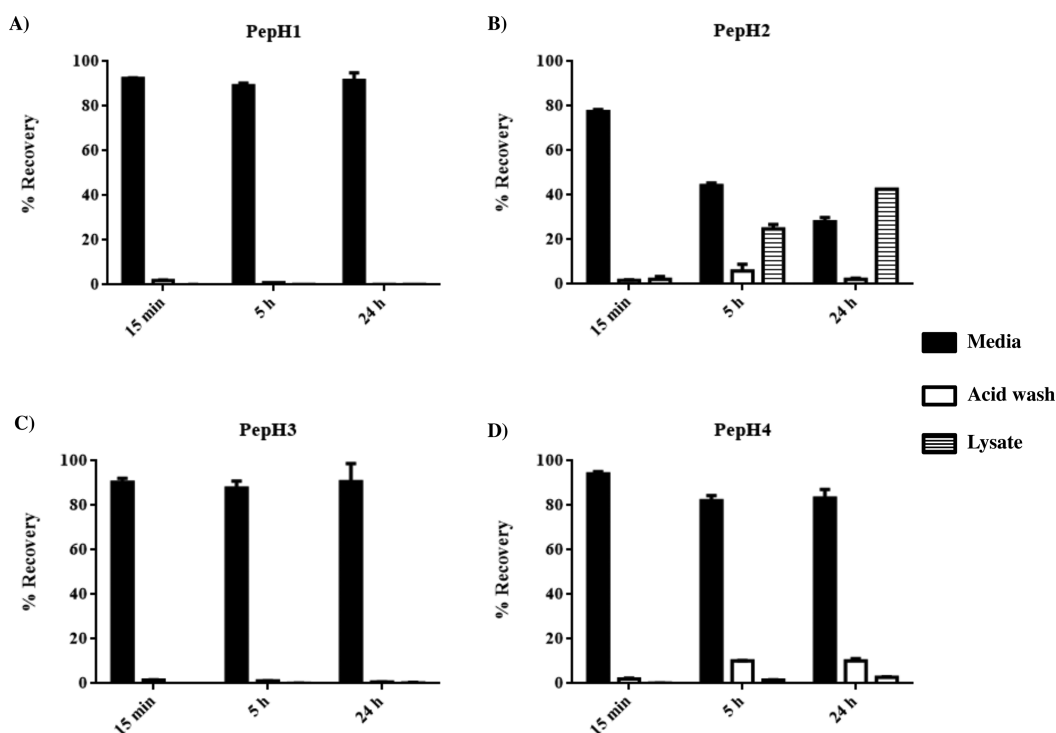


**Figure 4.** Radiopeptide uptake by bEnd.3 cells. The relative amount of non-bound radiopeptides in solution (black bars) and released from cells treated with acid buffer (membrane adsorption assay; white bars) and in cell lysate (internalization; striped bar) was determined for radiopeptides (TcPz<sup>x</sup>PepH1 to TcPz<sup>x</sup>PepH4, x = 1 or 2): PepH1 (A), PepH2 (B), PepH3 (C), and PepH4 (D), at 15 min and 5 and 24 h after peptide addition. The radioactivity intensity was normalized to the initial value added to cells and expressed as a percentage of recovery. PepH1 and PepH3 had no interaction with the cell membrane or internalization (lower than 0.6 and 0.4% at 24 h, respectively), while PepH2 showed strong interaction with cell membrane at 5 h (5.95%) and high internalization at 24 h (42.7%). PepH4 has moderate membrane interaction and low internalization (10.23 and 2.83% at 24 h, respectively). Values obtained from triplicates of two independent experiments.

**Table 2. Determination of BEB Translocation, Membrane Adsorption and Internalization of Radiopeptides in bEnd.3 Cells<sup>a</sup>**

peptide	recovered radioactivity in the base after 24 h (%)					
	BBB transmigration		membrane adsorption		internalization	
	TcPz <sup>x</sup>	GaNODA	TcPz <sup>x</sup>	GaNODA	TcPz <sup>x</sup>	GaNODA
PepH1	73.83 ± 9.40	71.47 ± 3.70	0.38 ± 0.10	0.62 ± 0.00	0.12 ± 0.00	0.16 ± 0.00
PepH2	9.32 ± 2.50	13.51 ± 0.70	2.20 ± 0.40	1.16 ± 0.10	42.70 ± 0.00	9.24 ± 1.20
PepH3	67.23 ± 1.20	72.63 ± 0.70	0.60 ± 0.10	0.60 ± 0.10	0.35 ± 0.20	0.30 ± 0.10
PepH4	63.45 ± 1.90	60.79 ± 2.60	10.23 ± 0.80	3.82 ± 0.10	2.83 ± 0.20	1.55 ± 0.10

<sup>a</sup>Recovered radioactivity of peptides labeled with TcPz<sup>x</sup> or GaNODA after 24 h incubation, in the base.

(ii) unraveling the mechanism of translocation of the most efficient domain peptide. Barrier translocation is a multistep vectorial process, starting with interaction with the membranes of cells on one side and exit of the cell on the other side, a process known as transcytosis. The interaction with the membranes may be receptor-mediated (receptor-mediated transcytosis, RMT) or consist of simple adsorption (adsorptive-mediated transcytosis, AMT). In both cases, RMT or AMT, efficient translocation across the barrier demands low entrapment inside cells. In this sense, not all cell-penetrating peptides are good translocators of cellular barriers and can be promising candidates to be used as BBB-crossing vectors. Cell-penetrating peptides that accumulate inside cells are not only low efficacy translocators but they also tend to accumulate in different organs and lead to undesired off-target effects. A study by Sarko *et al.*,<sup>39</sup> for instance, has shown that a panel of cell-penetrating peptides, including penetratin, Tat, pVEC, R<sub>9</sub>, and SynB<sub>1</sub>, accumulate unspecifically in different cell lines

(SW1736, PC3, MH wt, HNO 97, MCF7, and HCT 116) and, consequently, in different organs, such as heart and lung.<sup>39</sup>

In the present study, we have used a judicious combination of biophysical approaches in lipid vesicles, cellular models of the BEB, and *in vivo* biodistribution studies to ascertain which of the DEN2C specific peptide domains shows the most promising properties to be used as a trans-BBB peptide vector. All peptides were used in concentrations not toxic to the bEnd.3 cells as demonstrated in the *in vitro* model of the BEB (Figure 2) and viability assays (Figure S3). Radiolabeled PepH1 and PepH3 peptides showed efficient translocators of the BEB, reaching equal distribution of peptides over the two compartments of the transwell setup 24 h after application at the apical side (Figure 3). In contrast, PepH2 heavily associates to cellular membranes and accumulates inside cells, concomitantly not being an efficient BBB translocator. PepH4 showed an efficient BEB translocation; nevertheless, the data also demonstrated that it had moderate membrane retention and higher

Table 3. Biodistribution Profiles of  $^{99m}\text{Tc}(\text{CO})_3$ -labeled Peptide Vectors and Small Domain Antibody FC5<sup>a</sup>

organ	percentage of injected dose per gram of tissue (%ID/g)							
	TcPz <sup>3</sup> (control)		TcPz <sup>1</sup> PepH1		TcPz <sup>1</sup> PepH3		TcFC5	
	5 min	1 h	5 min	1 h	5 min	1 h	5 min	1 h
blood	3.60 ± 0.20	0.23 ± 0.01	2.90 ± 0.90	0.40 ± 0.20	8.60 ± 0.90	0.43 ± 0.04	6.00 ± 0.40	1.00 ± 0.20
liver	12.90 ± 0.60	5.00 ± 0.60	10.70 ± 1.90	3.00 ± 1.20	18.80 ± 6.10	2.30 ± 0.20	21.00 ± 0.80	12.40 ± 0.40
intestine	2.40 ± 0.40	10.00 ± 1.40	4.60 ± 0.80	11.50 ± 1.50	1.40 ± 0.20	23.0 ± 7.90	3.50 ± 0.30	0.79 ± 0.04
spleen	0.75 ± 0.01	0.40 ± 0.20	0.80 ± 0.20	0.90 ± 0.20	1.60 ± 0.40	0.18 ± 0.01	4.60 ± 2.00	4.20 ± 0.80
heart	1.17 ± 0.07	0.70 ± 0.50	0.70 ± 0.20	0.13 ± 0.02	2.20 ± 0.30	0.14 ± 0.01	4.20 ± 0.80	0.76 ± 0.03
lung	2.00 ± 0.40	0.40 ± 0.30	3.30 ± 0.60	1.70 ± 0.40	4.48 ± 0.01	0.31 ± 0.03	16.10 ± 6.50	38.20 ± 6.20
kidney	21.10 ± 4.00	2.70 ± 0.40	7.20 ± 1.10	1.40 ± 0.50	23.10 ± 3.40	3.50 ± 0.70	20.80 ± 3.90	96.40 ± 6.80
muscle	0.68 ± 0.07	0.20 ± 0.06	0.50 ± 0.20	0.12 ± 0.01	1.40 ± 0.20	0.20 ± 0.10	0.90 ± 0.10	0.39 ± 0.04
bone	0.70 ± 0.10	0.19 ± 0.08	0.60 ± 0.10	0.10 ± 0.03	1.89 ± 0.04	0.19 ± 0.01	1.60 ± 0.10	0.80 ± 0.30
stomach	1.40 ± 0.50	0.32 ± 0.15	0.50 ± 0.30	0.24 ± 0.06	1.10 ± 0.20	5.20 ± 0.70	1.90 ± 0.30	0.80 ± 0.30
brain	0.09 ± 0.01	0.04 ± 0.01	0.14 ± 0.03	0.02 ± 0.01	0.31 ± 0.07	0.03 ± 0.01	0.47 ± 0.27	0.07 ± 0.02
excretion (%ID)	11.60 ± 3.70	42.80 ± 7.60	20.20 ± 5.30	55.10 ± 11.00		36.00 ± 11.20		9.60 ± 1.40

<sup>a</sup>Tissue distribution of TcPz<sup>3</sup>, TcPz<sup>1</sup>PepH1, TcPz<sup>1</sup>PepH3, and TcFC5 at 5 min and 1 h post injection *via* tail vein in CD1 mice. Results are expressed as the average of percentage of injected dose (ID) per gram of tissue (%ID/g tissue; mean ± SD), *n* = 3.

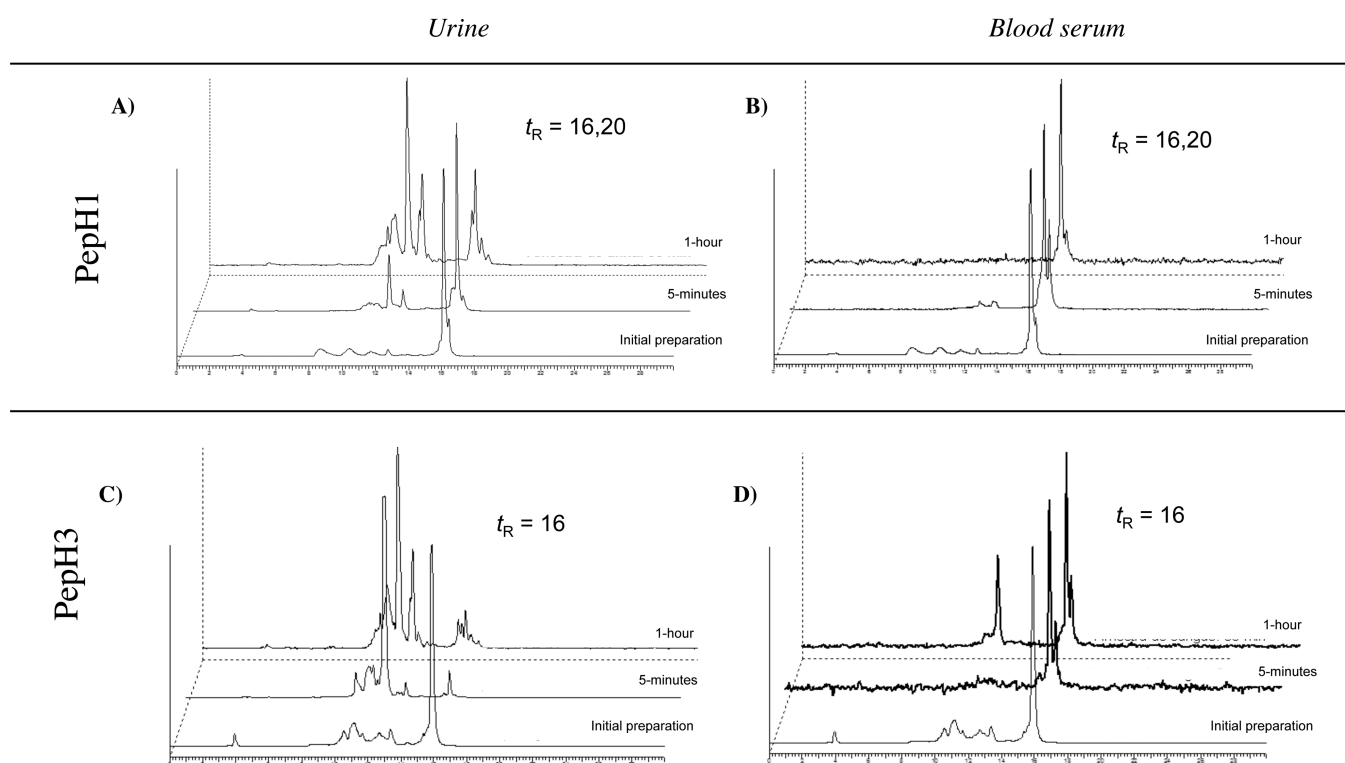


Figure 5. Chemical stability of  $^{99m}\text{Tc}(\text{CO})_3$ -labeled PepH1 and PepH3 in blood and urine. RP-HPLC  $\gamma$  traces of radiopeptides in blood serum (A and C) and urine samples (B and D) collected after 5 min and 1 h after injection.

internalization when compared with PepH1 and PepH3 (Figures 3 and 4).

The ability to discriminate the anionic lipid PS on the surface of cells may explain these results in part. PepH2 has increased affinity for zwitterionic POPC and POPC:Chol lipid bilayers in contrast with PepH3, which has the highest affinity for anionic POPC:POPS (1:4) bilayers (Supporting Information Figures S1 and S2). Ribeiro *et al.* showed that BECs are anionic, this being the key to the increased permeability of the BBB to cationic molecules.<sup>40</sup> BEC membranes are more anionic than the membranes of blood cells (red blood cells, RBC; peripheral blood mononuclear cells, PBMCs; and platelets) and other endothelial cells (human umbilical vascular endothelial cells, HUVEC).<sup>40</sup> BECs are relatively rich in PS and phosphatidy-

linositol, PI,<sup>41</sup> which makes PepH3 a very strong candidate to translocate the BBB. This ability to screen for PS may be the key to the differences in BBB translocation efficiency as both PepH2 and PepH3 have similar hydrophobicity ( $P_{o/w}$ , Table 1) and adopt the same conformation in lipid membranes. Lipid-membrane-induced acquisition of secondary-level structure in peptides positively correlates with propensity to translocate cell membranes.<sup>42,43</sup> Again, our results reveal that both hydrophobic peptides, PepH2 and PepH3, interact with bEnd.3 cell membranes, followed by internalization in the cell, yet their intercellular traffic pathway appears to be different, with PepH3 presenting high capacity to be delivered to the opposite side of the cell. However, PepH2 accumulates inside bEnd.3 cells. Molecular interaction with the cell membrane is thus a

necessary, but not sufficient, condition for BBB translocation to occur. In fact, not all molecules that interact with membranes are cell-penetrating and not all cell-penetrating molecules are able to translocate cellular barriers. Therefore, hydrophobicity increases propensity of a peptide to interact with membranes but cannot be used to predict cell penetration or cell translocation.

It is worth mentioning that PepH3 BEB translocation is consistent with AMT. It is known that AMT is triggered by electrostatic interaction between polycationic molecules and anionic microdomains in BECs.<sup>44</sup> Our data show that PepH3, a polycationic peptide, interacts electrostatically with anionic cell membranes. Another result consistent with AMT is the fast kinetics of translocation: compared to RMT, AMT involves lower binding affinity but higher binding capacity,<sup>45</sup> which grants faster kinetics to the translocation.

Altogether, the *in vitro* data demonstrated that PepH1 and PepH3 were the most promising peptides and were therefore selected to be further studied in the *in vivo* biodistribution. The *in vivo* data showed that brain uptake was very fast (up to 5 min post injection) and efficient (up to  $0.31 \pm 0.07\%$  ID/g for TcPz<sup>1</sup>PepH3), followed by a rapid brain washout ( $<0.03 \pm 0.01\%$  ID/g after 1 h) and clearance from blood, liver, kidney, and highly irrigated organs (Table 3). Taking into consideration that brain uptake higher than 0.1% ID/g has been accepted as the percentage of base limit for existing BBB crossing,<sup>46</sup> PepH3 demonstrated a potent brain targeting, achieving in some cases higher values than the ones obtained for known peptides designed for brain-targeted delivery. For instance, the peptides amylin, insulin, PYY3-36, and secretin present a brain uptake between 0.045 and 0.176% ID/g.<sup>47–50</sup> The angiopeptides family<sup>51</sup> has similar brain penetration when compared with PepH3 (0.18–0.6% ID/g), yet this penetration degree was obtained through *in situ* brain perfusion in contrast with injection in the tail vein, a much more demanding condition. Other “high performance” BBB peptide vectors such as TAT, penetratin, synB1, and others range from 0.2 to 0.9% ID/g of tissue.<sup>39</sup> The synthetic peptide K16ApoE presents the highest value of brain uptake, up to 1.14% ID/g.<sup>52</sup> In addition, antibodies that engage active RMT processes show similar translocation levels to PepH3<sup>17</sup> as observed for our control, FC5 ( $0.47 \pm 0.27\%$  ID/g). Furthermore, PepH3 is rapidly excreted in high percentages ( $36.0 \pm 11.2\%$  ID/g) when compared with FC5 ( $9.6 \pm 1.4\%$  ID/g), which is extremely positive to avoid toxic effects associated with accumulation in the brain. This property ensures that the peptide can be used as an active shuttle in and out of the brain, not only as an active carrier to the brain. In neurodegeneration therapy, for instance, removing cytotoxic aggregates from the brain may be as important as delivering drugs to the brain. The existence of molecular shuttles that are fit for both functions would be a major step forward for innovative therapeutic approaches. Our study paves the way for new strategies in CNS-targeted therapies.

**Conclusion.** Results of *in vitro* and *in vivo* assays have shown that selected DEN2C-derived peptides have a high ability to cross the BBB. There is strong evidence that PepH3 efficiently penetrates the brain using AMT and returns to blood circulation to be excreted. Thus, PepH3 is a potential trans-BBB shuttle,<sup>53</sup> potentially able to carry drugs from the blood to brain and toxic cargo from the brain to blood, which may lead to new therapeutic applications in the CNS field,<sup>54</sup> such as Alzheimer’s or Parkinson diseases.

## METHODS

Peptide sequences were selected from particular domains of the Dengue virus capsid protein (helical domains, underlined and listed in Table 1), with the following sequence:

MNDQRKKARNTPFNMLKRENRNRVSTVQQLTKR-FSLGMLQGRGPKLFLMALVAFLRFLTIPPTAGILKRWGT-IKKSKAINVLRGRFKEIGRMLNILNRRRR.

The FC5 antibody fragment<sup>16,55</sup> was synthesized by Nzytech (Lisbon, Portugal).

**Materials.** All N- $\alpha$ -Fmoc-protected amino acids, MBHA rink amide resin, O-(benzotriazol-1-yl)-N,N,N',N'-tetramethyluronium hexafluorophosphate (HBTU), and N-[(dimethylamino)-1H-1,2,3-triazolo-[4,5-b]pyridin-1-ylmethylene]-N-methylmethanaminium hexafluorophosphate N-oxide (HATU) were purchased from Novabiochem (Merck, Lisbon, Portugal).

4-((3-(4-(2-*tert*-Butoxy-2-oxoethyl)-3,5-dimethyl-1H-pyrazol-1-yl)ethyl)(2-*tert*-butoxycarbonylamino)ethyl)amino)butanoic acid (*t*-BuPz<sup>1</sup>(Boc)) and 1-(2-((2-*tert*-butoxycarbonylamino)ethyl)(3-carboxypropyl)amino)ethyl)-1H-pyrazole-4-carboxylic acid (Pz<sup>2</sup>(Boc)) were synthesized as described in Morais *et al.*<sup>56</sup> The macrocyclic bifunctional chelator 4-(4,7-bis(2-(*tert*-butoxy)-2-oxoethyl)-1,4,7-triazacyclononan-1-yl)-5-(*tert*-butoxy)-5-oxopentanoic acid (NODA-GA(*t*Bu)<sub>3</sub>) was purchased from CheMatech (Dijon, France). 1-Palmitoyl-2-oleoyl-*sn*-glycero-3-phosphocholine (POPC), 1-palmitoyl-2-oleoyl-*sn*-glycero-3-phosphocholineserine (POPS), 1-palmitoyl-2-oleoyl-*sn*-glycero-3-phospho-(19-*sn*-glycerol) (POPG), and cholesterol were obtained from Avanti Polar Lipids (Netherlands). 4-(2-[6-(Diocylamino)-2-naphthalenyl]ethenyl)-1-(3-sulfopropyl)-pyridinium (di-8-ANEPPS) was obtained from Molecular Probes (Eugene, OR).

The cell lines and media were obtained from American Type Culture Collection (ATCC, Manassas, USA). Fibronectin bovine plasma was obtained from CALBIOCHEM. Other consumables used in the *in vitro* assays were purchased from Gibco-Invitrogen. Tissue culture inserts and 24-well plates were obtained from BD falcon. All other chemicals and solvents were obtained from either Merck or Sigma-Aldrich.

Sodium pertechnetate ( $\text{Na}^{[99\text{mTcO}_4]}$ ) was eluted from a <sup>99</sup>Mo/<sup>99m</sup>Tc generator, using 0.9% saline. The precursor *fac*- $^{[99\text{mTc}}(\text{CO})_3(\text{H}_2\text{O})_3]^+$  was prepared using an Isolink kit and its radiochemical purity checked by RP-HPLC as previously described.<sup>56</sup>

Gallium-67 citrate (<sup>67</sup>Ga-citrate) was a gift from the nuclear medicine service of Hospital de Santa Maria (Lisbon, Portugal). <sup>67</sup>GaCl<sub>3</sub> was prepared from <sup>67</sup>Ga-citrate (Mallinckrodt Medical, Netherlands) as described in the literature.<sup>57</sup>

**Reverse Phase High Performance Liquid Chromatography (RP-HPLC) analysis.** HPLC analyses were performed on a PerkinElmer LC pump 200 coupled to a Shimadzu SPD 10AV UV/vis and to a Berthold-LB 509 radiometric detector.

Analytical control and semipreparative purifications of the peptides and peptide conjugates were achieved on a Supelco Discovery Bio Wide Pore C18 column (250 mm × 4.6 mm, 5  $\mu\text{m}$ ) and Supelco Discovery Bio Wide Pore C18 column (250 mm × 10 mm, 10  $\mu\text{m}$ ) with a flow rate of 1.0 mL min<sup>-1</sup> or 2.0 mL min<sup>-1</sup> (gradient B), respectively. In both cases, UV detection was as follows:  $\lambda = 220$  and 280 nm. Eluents: A, 0.1% TFA in H<sub>2</sub>O; B, 0.1% TFA in CH<sub>3</sub>CN.

**Applied Binary HPLC Gradients.** Gradient A (PepH1, PepH3, and corresponding conjugates): 0–25 min, 10–50% B; 25–27 min, 100% B; 27–28 min, 100–0% B; 28–30 min, 10% B.

Gradient B (PepH2 and corresponding conjugate): 0–5 min, 50% B; 5–30 min, 50–100% B; 30–35 min, 100% B; 35–36 min, 100–50% B; 36–40 min, 50% B.

Gradient C (PepH4 and corresponding conjugate): 0–25 min, 10–70% B; 25–27 min, 100% B; 27–28 min, 100–0% B; 28–30 min, 10% B.

Gradient D (<sup>99m</sup>Tc-labeled peptide conjugates): 0–3 min, 0% B; 3–3.1 min, 0–25% B; 3.1–9.0 min, 25% B; 9.0–9.1 min, 25–34% B; 9.1–14.1 min, 34–100% B; 14.1–19.0 min, 100% B; 19.0–21.0 min, 100% B; 21–30 min, 0% B.



Gradient E ( $^{67}\text{Ga}$ -labeled peptide conjugates): 0.0–3.0 min, 0% B; 3.0–3.1 min, 0–10% B; 3.1–19.9 min, 10–100% B; 19.9–22.0 min, 100% B; 22.0–23.0 min; 100–0%; 23.0–30.0 min, 0% B.

**Synthesis of the Peptides.** The peptides (Table 1) were assembled on Rink Amide MBHA resin by Fmoc-based solid phase peptide synthesis (SPPS) in a CEM 12-channel microwave assisted automated peptide synthesizer (Liberty). After cleavage from the resin, semipreparative RP-HPLC purification, and lyophilization (following gradients described above), the peptides were obtained as white solids. Finally, the peptides were characterized by electrospray ionization mass spectrometry (ESI-MS) and their concentration determined by UV spectrophotometry.

**Synthesis of the Peptide Conjugates.** The peptide-conjugates  $\text{Pz}^x\text{PepHY}$  ( $x = 1$  or  $2$ ;  $Y = 1$ – $4$ ) were prepared in solid support by conjugation of  $t$ - $\text{buPz}^1(\text{Boc})$ ,  $\text{Pz}^2(\text{Boc})$ , or  $\text{NODA-GA}(t\text{Bu})_3$  to the N-terminal of each peptide sequence. Briefly, the protected chelating agent (2.5 equiv per amine on resin) was preincubated for 5 min with hydroxybenzotriazole (HOBt; 1.2 equiv per carboxylate) and benzotriazole-1-yl-oxy-tris-pyrrolidino-phosphonium hexafluorophosphate (PyBop; 1.2 equiv per carboxylate). This solution was added to the peptidyl resin (ca. 50 mg) previously suspended in dimethylformamide (DMF) and  $N,N$ -diisopropylethylamine (DIPEA; 1 equiv per amine group). After stirring for 2 h at RT, the solvents were removed by filtration, and the resin was washed with DMF (3 $\times$ ),  $\text{CH}_2\text{Cl}_2$  (3 $\times$ ), DMF (3 $\times$ ), and  $\text{CH}_2\text{Cl}_2$  (3 $\times$ ).

Removal of the protecting group as well as cleavage of the peptide conjugates from the resin was performed using a standard cleavage cocktail (95% TFA, 2.5% TIS, 2.5%  $\text{H}_2\text{O}$ ). After stirring for 2 h at RT, the TFA solution was collected after removal of the resin by filtration. The solution was concentrated, and the conjugate was precipitated with ice-cold diethyl ether. The solid was washed several times with ice-cold diethyl ether and dried under a nitrogen flow before lyophilization. The lyophilized peptide conjugates were dissolved in 10% (v/v) acetic acid solution and purified by semipreparative RP-HPLC to yield the desired peptide conjugates that were characterized by ESI-MS and lyophilized.

**Radiolabeling with  $^{99m}\text{Tc}(\text{CO})_3^+$ .** The radiopeptides  $\text{TcPz}^x\text{PepHY}$  ( $x = 1$  or  $2$ ;  $Y = 1$ – $4$ ) were synthesized by reaction of the peptide conjugates  $\text{Pz}^x\text{PepHY}$  ( $x = 1$  or  $2$ ;  $Y = 1$ – $4$ ) with the precursor  $\text{fac-}^{99m}\text{Tc}(\text{CO})_3(\text{H}_2\text{O})_3^+$ , which was prepared using an Isolink kit and its radiochemical purity checked by RP-HPLC. Briefly, a solution of  $\text{fac-}^{99m}\text{Tc}(\text{CO})_3(\text{H}_2\text{O})_3^+$  (900  $\mu\text{L}$ ) was added to a capped vial previously flushed with  $\text{N}_2$ , containing a solution of peptide conjugate (100  $\mu\text{L}$ , 1 mM). The mixture reacted for 30 min at 100  $^\circ\text{C}$ , and the radiochemical purity of the radiopeptides was checked by RP-HPLC (gradient D). The radiolabeled compound was purified by semipreparative RP-HPLC (gradient D). The activity corresponding to  $\text{TcPz}^x\text{PepHY}$  ( $x = 1$  or  $2$ ;  $Y = 1$ – $4$ ) was collected in a 50 mL Falcon flask, containing 200  $\mu\text{L}$  of PBS with 0.2% BSA, and purged with  $\text{N}_2$  gas to remove the acetonitrile. The pH of the final solution was adjusted to 7.4 with 0.1 M NaOH for the cell studies. The final product was controlled by analytical RP-HPLC (gradient D). The control model complex  $\text{TcPz}^3$  was prepared as described by Alves *et al.*<sup>58</sup> In brief,  $\text{TcPz}^3$  was obtained upon reaction of the bifunctional chelator  $\text{Pz}^3$  (4-((2-aminoethyl)(2-(3,5-dimethyl-1H-pyrazolyl-1-yl)-ethyl)amino)butanoic acid) with  $\text{fac-}^{99m}\text{Tc}(\text{CO})_3(\text{H}_2\text{O})_3^+$  at 100  $^\circ\text{C}$  for 30 min.

**Radiolabeling with  $^{67}\text{Ga}^{3+}$ .** The pH of a fraction (0.5 mL) of  $^{67}\text{GaCl}_3$  eluted from a SEP-PAK cartridge was adjusted to pH 5 by adding sodium acetate (18 mg). Part of this solution (190  $\mu\text{L}$ , 370–420 MBq) was added to the peptide conjugate (10  $\mu\text{L}$ , 1 mM), and the mixture was incubated for 5 min at RT. The radiochemical purity of the radiopeptides  $^{67}\text{Ga-NODAGA-PepHY}$  ( $\text{GaNODAGAPepHY}$ ,  $Y = 1$ – $4$ ) was checked by RP-HPLC (gradient E).

**Partition Coefficient.** The octanol–water partition coefficient was evaluated by the “shake-flask” method.<sup>31</sup> Briefly, the radiopeptide conjugate was added to a mixture of octanol (1 mL) and 0.1 M PBS at pH 7.4 (1 mL), previously saturated with each other by stirring. This mixture was vortexed and centrifuged (300 rpm, 10 min) to allow phase separation. Aliquots of both octanol and PBS were counted in a

$\gamma$  counter. The partition coefficient ( $P_{o/w}$ ) was calculated by dividing the counts in the octanol phase by those in the buffer.

**Cell Culture.** bEnd.3 brain endothelioma cells (ATTCC-CRL-2299, Lot. 59618606) were grown in DMEM supplemented with 10% fetal bovine serum (FBS) and 1% penicillin/streptomycin antibiotic solution. Cells were cultured in a humidified atmosphere of 95% air and 5%  $\text{CO}_2$  at 37  $^\circ\text{C}$  (MCO-19AIC (UV), Sanyo), with the medium changed every other day. The cells were adherent in monolayers and, when confluent, were harvested from cell culture flasks with trypsin EDTA and seeded 3000 cells/well to fibronectin bovine plasma coated tissue culture inserts (pore size of 1  $\mu\text{m}$ ) for 24-well plates (BD falcon). To allow to form tight junctions and to have a stable *in vitro* model, cells were grown for 9 days and the media changed every 2 days. Conditions were optimized from protocols described by others.<sup>59</sup>

**BEB Integrity Assays.** A total of 1  $\mu\text{M}$  of each unlabeled peptide solution in complete media was added to bEnd.3 cells grown in tissue culture inserts (for 9 days, as described before) and incubated for 24 h. After incubation, peptide solution was removed and cells washed once with PBS and three times with transport buffer (5 mM glucose, 5 mM  $\text{MgCl}_2$ , 10 mM HEPES at pH 7.4, and 0.05% BSA). Fluorescent probes of 5(6)-carboxyfluorescein (FITC) with a molecular weight (MW) of 376.32 Da and fluorescein isothiocyanate-dextran with a MW of 4 and 40 kDa (FD4 and FD40, respectively; all from Sigma-Aldrich), were diluted in transport buffer to an absorbance of 0.1, from stocks of 25 mg  $\text{mL}^{-1}$ . Probes were then added to the apical side (apex) and incubated for 2 h. Samples were collected from apex and base, and fluorescence intensity was measured at  $\lambda$  with an excitation of 493 nm and maximum emission at 560 nm in a plate reader (TECAN infinity M200).

**BEB *In Vitro* Model of Translocation and Cellular Internalization.** A total of 5  $\mu\text{Ci mL}^{-1}$  of the radiopeptides was added to bEnd.3 cells grown in tissue culture inserts and incubated for different time points (15 min, 5 and 24 h). After incubation, samples were collected from apex, base, and membrane. In addition, both base and apex were washed with 10% DMSO in PBS. The washing samples were combined to the respective sample from the apical side and the base. The radioactivity in the samples collected from the apical side, base, and in the filter were measured in a  $\gamma$  counter (LB211, Berthold, Germany).

For the internalization and cellular interaction studies, 5  $\mu\text{Ci mL}^{-1}$  of radiopeptides were added to bEnd.3 cells growing in 24-well plates and incubated for 15 min, 5 h, and 24 h. After incubation, cells were washed with cold media, followed by two acid washes (50 mM glycine, 100 mM NaCl, pH 2.8). After neutralization with PBS, cells were lysed (lysis buffer: 1 M NaOH) and the cellular content collected. The radioactivity associated with each fraction was measured in the  $\gamma$  counter.

**FC5 Antibody Domain Preparation.** DNA encoding the FC5 clone was synthesized by Nzytech, adding a NheI and XhoI restriction sites at the 5' and 3' ends, respectively, for cloning into pET21a(+) or pET28a plasmid (Novagen, Merck Millipore). A fragment encoding FC5-HIS-HA was generated by PCR (KOD Hot start Master Mix, Merck Millipore) and then purified (QIAquick Gel extraction Kit, Qiagen), followed by insertion into the expression vector. The expression vector containing the gene of interest was then transformed into bacterial strain BL21(DE3) (Nzytech). An isolated colony with a gene of interest (confirmed by sequencing) was used to prepare stocks and to express the protein in selective media (super broth (SB) containing ampicillin). Protein expression was induced by the addition of 1 mM isopropyl 1-thiol- $\beta$ -D-galactopyranoside (IPTG) to a culture with  $A_{600\text{ nm}} = 0.6$  at 37  $^\circ\text{C}$ ; after induction, the bacteria were grown 16 h at 16  $^\circ\text{C}$ . Cells were harvested by centrifugation and resuspended in 50 mM sodium phosphate, 1 M sodium chloride, and 10% glycerol, at pH 6.8. The pellet was sonicated at 4  $^\circ\text{C}$  for 20 min and centrifuged at 10 000 rpm for 30 min, at 4  $^\circ\text{C}$ . Supernatant was purified by immobilized metal affinity chromatography (IMAC), using HP HisTrap columns and the AKTA FPLC system (GE Healthcare). After purification, the purity (>95%) of the eluted samples was analyzed by sodium dodecyl sulfate-polyacrylamide gel electrophoresis (SDS-PAGE).

**Radiolabeling of FC5 Antibody Domain.** The radiolabeled protein  $^{99m}\text{Tc}(\text{CO})_3\text{-FC5}$  (TcFC5) was prepared by reacting the recombinant antibody with  $\text{fac-}[^{99m}\text{Tc}(\text{CO})_3(\text{H}_2\text{O})_3]^+$ . Briefly, a specific volume of the  $\text{fac-}[^{99m}\text{Tc}(\text{CO})_3(\text{H}_2\text{O})_3]^+$  solution was added to a nitrogen-purged closed glass vial containing a solution of the His-tag containing FC5 VHH antibody in order to get a final concentration of  $1 \text{ mg mL}^{-1}$ . In order to avoid undesired aggregation of the protein, an adequate volume of a 10% SDS solution was added in order to reach a final concentration of 0.5%. The mixture reacted for 30 min at  $37^\circ\text{C}$ , and the radiochemical purity of TcFC5 was checked by instant thin-layer chromatography silica gel (ITLC-SG, Varian) analysis using a 5% HCl (6 M) solution in MeOH as the eluent.  $[\text{fac-}[^{99m}\text{Tc}(\text{CO})_3(\text{H}_2\text{O})_3]^+$  and  $[\text{TcO}_4]^-$  migrate in the front of the solvent ( $R_f = 1$ ), whereas the radioactive antibody remains at the origin ( $R_f = 0$ ). Radioactivity distribution on the ITLC-SG strips was detected by a radioactive scanner (Berthold LB 2723, Germany) equipped with a 20 mm diameter NaI(Tl) scintillation crystal. Purification of the  $^{99m}\text{Tc}$ -labeled antibody was performed using Amicon (10 K, Merck Millipore) centrifugal filters for protein purification and concentration following the procedure of the supplier. The supernatant is discarded, and the pellet containing TcFC5 was resuspended in  $100 \mu\text{L}$  of PBS and used in the biodistribution studies in mice. The radiochemical purity (>95%) was determined by ITLC-SG.

**Biodistribution.** All animal experiments were performed in compliance with national and European regulations for animal experimentation. The animals were housed in a temperature and humidity controlled room with a 12 h light/12 h dark schedule. Biodistribution of radiopeptides was performed on CD1 mice.

Animals were intravenously injected into the tail vein with the radiolabeled compound diluted in  $100 \mu\text{L}$  of PBS at pH 7.2 (TcPz<sup>3</sup>, ca. 6.5 MBq/mouse, ca. 1911 MBq/mg; TcPz<sup>1</sup>PepH1, ca. 6.9 MBq/mouse, 60 MBq/mg; TcPz<sup>1</sup>PepH3, ca. 0.4 MBq/mouse, ca. 3.1 MBq/mg; TcFC5, ca. 3.8 MBq/mouse). The mice were sacrificed by cervical dislocation at 5 min and 1 h after injection. The dose was administered and the radioactivity in the sacrificed animals was measured using a dose calibrator (Carpintec CRC-15W, Ramsey, USA). The difference between the radioactivity in the injected and the euthanized animals was assumed to be due to excretion. Brain and tissues of interest were dissected, rinsed to remove excess blood, and weighed, and their radioactivity was measured using a  $\gamma$  counter. The uptake in the brain and tissues of interest was calculated and expressed as a percentage of injected radioactivity dose per gram of tissue (% ID/g).

**In Vivo Stability.** The stability of the complexes was assessed by RP-HPLC analysis of urine and blood serum, under identical conditions to those used to analyze the original radiopeptides. The samples were collected 5 min and 1 h after injection. The urine collected at the time of sacrifice and filtered through a Millex GV filter ( $0.22 \mu\text{m}$ ) before analysis. Blood collected from mice was centrifuged at 3000 rpm for 15 min at  $4^\circ\text{C}$  and the serum separated. The serum was treated with ethanol in a 2:1 (v/v) ratio to precipitate the proteins. After centrifugation, the supernatant was collected and analyzed by RP-HPLC.

## ■ ASSOCIATED CONTENT

### ● Supporting Information

The Supporting Information is available free of charge on the ACS Publications website at DOI: 10.1021/acscchembio.7b00087.

Figures S1 and S2, biophysical studies of peptide interaction with membrane models; Figure S3, results of cell viability assays; Table S1, percentage of transmigration of the transwell cellular BBB model and cellular adsorption and internalization at 15 min and 5 and 24 h; supplemental experimental procedures (PDF)

## ■ AUTHOR INFORMATION

### Corresponding Author

\*E-mail: [macastanho@medicina.ulisboa.pt](mailto:macastanho@medicina.ulisboa.pt).

### ORCID

Vera Neves: 0000-0002-2989-7208

Miguel A. R. B. Castanho: 0000-0001-7891-7562

### Notes

The authors declare no competing financial interest.

## ■ ACKNOWLEDGMENTS

The authors thank the Portuguese Funding Agency, Fundação para a Ciência e a Tecnologia, FCT IP, for financial support (grants SFRH/BPD/94466/2013; SFRH/BPD/109010/2015; IF/01010/2013; PTDC/BBNAN/1578/2014; HIVERA/0002/2013) and Marie Skłodowska-Curie Research and Innovation Staff Exchange (MSCA-RISE), call 20-MSCA-RISE-2014 (grant agreement H20 644167 – INPACT). M.M., L.G., C.F., and J.D.G.C. gratefully acknowledge FCT support through the UID/Multi/04349/2013 project.

## ■ REFERENCES

- (1) (2006) *Neurological Disorders: Public Health Challenges*, WHO Press, Switzerland.
- (2) Neuwelt, E., Abbott, N. J., Abrey, L., Banks, W. A., Blakley, B., Davis, T., Engelhardt, B., Grammas, P., Nedergaard, M., Nutt, J., Pardridge, W., Rosenberg, G. A., Smith, Q., and Drewes, L. R. (2008) Strategies to advance translational research into brain barriers. *Lancet Neurol.* 7, 84–96.
- (3) Guo, L., Ren, J., and Jiang, X. (2012) Perspectives on brain-targeting drug delivery systems. *Curr. Pharm. Biotechnol.* 13, 2310–8.
- (4) Pardridge, W. M. (2007) Blood-brain barrier delivery. *Drug Discovery Today* 12, 54–61.
- (5) Neuwelt, E. A., Bauer, B., Fahlke, C., Fricker, G., Iadecola, C., Janigro, D., Leybaert, L., Molnar, Z., O'Donnell, M. E., Povlishock, J. T., Saunders, N. R., Sharp, F., Stanimirovic, D., Watts, R. J., and Drewes, L. R. (2011) Engaging neuroscience to advance translational research in brain barrier biology. *Nat. Rev. Neurosci.* 12, 169–82.
- (6) Interlandi, J. (2013) Breaking the brain barrier. *Sci. Am.* 308, 52–7.
- (7) Patel, M. M., Goyal, B. R., Bhadada, S. V., Bhatt, J. S., and Amin, A. F. (2009) Getting into the brain: approaches to enhance brain drug delivery. *CNS Drugs* 23, 35–58.
- (8) Tamsamani, J., Rousselle, C., Rees, A. R., and Scherrmann, J. M. (2001) Vector-mediated drug delivery to the brain. *Expert Opin. Biol. Ther.* 1, 773–82.
- (9) Strazielle, N., and Ghersi-Egea, J. F. (2013) Physiology of blood–brain interfaces in relation to brain disposition of small compounds and macromolecules. *Mol. Pharmaceutics* 10, 1473–91.
- (10) Yu, Y. J., Zhang, Y., Kenrick, M., Hoyte, K., Luk, W., Lu, Y., Atwal, J., Elliott, J. M., Prabhu, S., Watts, R. J., and Dennis, M. S. (2011) Boosting brain uptake of a therapeutic antibody by reducing its affinity for a transcytosis target. *Sci. Transl. Med.* 3, 84ra44.
- (11) Yu, Y. J., Atwal, J. K., Zhang, Y., Tong, R. K., Wildsmith, K. R., Tan, C., Bien-Ly, N., Hersom, M., Maloney, J. A., Meilandt, W. J., Bumbaca, D., Gadkar, K., Hoyte, K., Luk, W., Lu, Y., Ernst, J. A., Scarce-Lavie, K., Couch, J. A., Dennis, M. S., and Watts, R. J. (2014) Therapeutic bispecific antibodies cross the blood–brain barrier in nonhuman primates. *Sci. Transl. Med.* 6, 261ra154.
- (12) Pardridge, W. M. (2002) Drug and gene targeting to the brain with molecular Trojan horses. *Nat. Rev. Drug Discov* 1, 131–9.
- (13) Ohshima-Hosoyama, S., Simmons, H. A., Goecks, N., Joers, V., Swanson, C. R., Bondarenko, V., Velotta, R., Brunner, K., Wood, L. D., Hruban, R. H., and Emborg, M. E. (2012) A monoclonal antibody-GDNF fusion protein is not neuroprotective and is associated with proliferative pancreatic lesions in parkinsonian monkeys. *PLoS One* 7, e39036.

- (14) Couch, J. A., Yu, Y. J., Zhang, Y., Tarrant, J. M., Fuji, R. N., Meilandt, W. J., Solanoy, H., Tong, R. K., Hoyte, K., Luk, W., Lu, Y., Gadkar, K., Prabhu, S., Ordonia, B. A., Nguyen, Q., Lin, Y., Lin, Z., Balazs, M., Searce-Levie, K., Ernst, J. A., Dennis, M. S., and Watts, R. J. (2013) Addressing safety liabilities of TfR bispecific antibodies that cross the blood–brain barrier. *Sci. Transl. Med.* *5*, 183ra57.
- (15) Farrington, G. K., Caram-Salas, N., Haqqani, A. S., Brunette, E., Eldredge, J., Pepinsky, B., Antognetti, G., Baumann, E., Ding, W., Garber, E., Jiang, S., Delaney, C., Boileau, E., Sisk, W. P., and Stanimirovic, D. B. (2014) A novel platform for engineering blood–brain barrier-crossing bispecific biologics. *FASEB J.* *28*, 4764–78.
- (16) Muruganandam, A., Tanha, J., Narang, S., and Stanimirovic, D. (2002) Selection of phage-displayed llama single-domain antibodies that transigrate across human blood–brain barrier endothelium. *FASEB J.* *16*, 240–2.
- (17) Zuchero, Y. J., Chen, X., Bien-Ly, N., Bumbaca, D., Tong, R. K., Gao, X., Zhang, S., Hoyte, K., Luk, W., Huntley, M. A., Phu, L., Tan, C., Kallop, D., Weimer, R. M., Lu, Y., Kirkpatrick, D. S., Ernst, J. A., Chih, B., Dennis, M. S., and Watts, R. J. (2016) Discovery of Novel Blood-Brain Barrier Targets to Enhance Brain Uptake of Therapeutic Antibodies. *Neuron* *89*, 70–82.
- (18) Georgieva, J. V., Kalicharan, D., Couraud, P. O., Romero, I. A., Weksler, B., Hoekstra, D., and Zuhorn, I. S. (2010) Surface characteristics of nanoparticles determine their intracellular fate in and processing by human blood–brain barrier endothelial cells in vitro. *Mol. Ther.* *19*, 318–325.
- (19) Herve, F., Ghinea, N., and Scherrmann, J. M. (2008) CNS delivery via adsorptive transcytosis. *AAPS J.* *10*, 455–72.
- (20) Drin, G., Cottin, S., Blanc, E., Rees, A. R., and Tamsamani, J. (2003) Studies on the internalization mechanism of cationic cell-penetrating peptides. *J. Biol. Chem.* *278*, 31192–201.
- (21) Lindgren, M., Gallet, X., Soomets, U., Hallbrink, M., Brakenhielm, E., Pooga, M., Brasseur, R., and Langel, U. (2000) Translocation properties of novel cell penetrating transportan and penetratin analogues. *Bioconjugate Chem.* *11*, 619–26.
- (22) Zou, L. L., Ma, J. L., Wang, T., Yang, T. B., and Liu, C. B. (2013) Cell-penetrating Peptide-mediated therapeutic molecule delivery into the central nervous system. *Curr. Neuropharmacol.* *11*, 197–208.
- (23) Rousselle, C., Clair, P., Lefauconnier, J. M., Kaczorek, M., Scherrmann, J. M., and Tamsamani, J. (2000) New advances in the transport of doxorubicin through the blood–brain barrier by a peptide vector-mediated strategy. *Mol. Pharmacol.* *57*, 679–686.
- (24) Schwarze, S. R., Ho, A., Vocero-Akbani, A., and Dowdy, S. F. (1999) In vivo protein transduction: delivery of a biologically active protein into the mouse. *Science* *285*, 1569–1572.
- (25) Thomas, F. C., Taskar, K., Rudraraju, V., Goda, S., Thorsheim, H. R., Gaasch, J. A., Mittapalli, R. K., Palmieri, D., Steeg, P. S., Lockman, P. R., and Smith, Q. R. (2009) Uptake of ANG1005, a novel paclitaxel derivative, through the blood–brain barrier into brain and experimental brain metastases of breast cancer. *Pharm. Res.* *26*, 2486–94.
- (26) Freire, J. M., Almeida Dias, S., Flores, L., Veiga, A. S., and Castanho, M. A. (2015) Mining viral proteins for antimicrobial and cell-penetrating drug delivery peptides. *Bioinformatics* *31*, 2252–6.
- (27) Ma, L., Jones, C. T., Groesch, T. D., Kuhn, R. J., and Post, C. B. (2004) Solution structure of dengue virus capsid protein reveals another fold. *Proc. Natl. Acad. Sci. U. S. A.* *101*, 3414–9.
- (28) Freire, J. M., Veiga, A. S., Conceicao, T. M., Kowalczyk, W., Mohana-Borges, R., Andreu, D., Santos, N. C., Da Poian, A. T., and Castanho, M. A. (2013) Intracellular nucleic acid delivery by the supercharged dengue virus capsid protein. *PLoS One* *8*, e81450.
- (29) Freire, J. M., Veiga, A. S., Rego de Figueiredo, I., de la Torre, B. G., Santos, N. C., Andreu, D., Da Poian, A. T., and Castanho, M. A. (2014) Nucleic acid delivery by cell penetrating peptides derived from dengue virus capsid protein: design and mechanism of action. *FEBS J.* *281*, 191–215.
- (30) Freire, J. M., Veiga, A. S., de la Torre, B. G., Santos, N. C., Andreu, D., Da Poian, A. T., and Castanho, M. A. (2013) Peptides as models for the structure and function of viral capsid proteins: Insights on dengue virus capsid. *Biopolymers* *100*, 325–36.
- (31) Troutner, D. E., Volkert, W. A., Hoffman, T. J., and Holmes, R. A. (1984) A neutral lipophilic complex of 99mTc with a multidentate amine oxime. *Int. J. Appl. Radiat. Isot.* *35*, 467–70.
- (32) Puerta-Guardo, H., Mosso, C., Medina, F., Liprandi, F., Ludert, J. E., and del Angel, R. M. (2010) Antibody-dependent enhancement of dengue virus infection in U937 cells requires cholesterol-rich membrane microdomains. *J. Gen. Virol.* *91*, 394–403.
- (33) Hu, K., Li, J., Shen, Y., Lu, W., Gao, X., Zhang, Q., and Jiang, X. (2009) Lactoferrin-conjugated PEG-PLA nanoparticles with improved brain delivery: in vitro and in vivo evaluations. *J. Controlled Release* *134*, 55–61.
- (34) Brown, R. C., Morris, A. P., and O’Neil, R. G. (2007) Tight junction protein expression and barrier properties of immortalized mouse brain microvessel endothelial cells. *Brain Res.* *1130*, 17–30.
- (35) Morais, M., Paulo, A., Gano, L., Santos, I., and Correia, J. D. G. (2013) Target-specific Tc(CO)<sub>3</sub>-complexes for *in vivo* imaging. *J. Organomet. Chem.* *744*, 125–139.
- (36) Veliky, I. (2014) Prospective of <sup>68</sup>Ga-Radiopharmaceutical Development. *Theranostics* *4*, 47–80.
- (37) Freire, J. M., Santos, N. C., Veiga, A. S., Da Poian, A. T., and Castanho, M. A. (2015) Rethinking the capsid proteins of enveloped viruses: multifunctionality from genome packaging to genome transfection. *FEBS J.* *282*, 2267–78.
- (38) Cruz-Oliveira, C., Freire, J. M., Conceicao, T. M., Higa, L. M., Castanho, M. A., and Da Poian, A. T. (2015) Receptors and routes of dengue virus entry into the host cells. *FEMS Microbiol. Rev.* *39*, 155–70.
- (39) Sarko, D., Beijer, B., Garcia Boy, R., Nothelfer, E. M., Leotta, K., Eisenhut, M., Altmann, A., Haberkorn, U., and Mier, W. (2010) The pharmacokinetics of cell-penetrating peptides. *Mol. Pharmaceutics* *7*, 2224–2231.
- (40) Ribeiro, M. M., Domingues, M. M., Freire, J. M., Santos, N. C., and Castanho, M. A. (2012) Translocating the blood–brain barrier using electrostatics. *Front. Cell. Neurosci.*, *6*, DOI: [10.3389/fncel.2012.00044](https://doi.org/10.3389/fncel.2012.00044).
- (41) Muhs, A., Hickman, D. T., Pihlgren, M., Chuard, N., Giriens, V., Meerschman, C., van der Auwera, L., van Leuven, F., Sugawara, M., Weingertner, M. C., Bechinger, B., Greferath, R., Kolonko, N., Nagel-Steger, L., Riesner, D., Brady, R. O., Pfeifer, A., and Nicolau, C. (2007) Liposomal vaccines with conformation-specific amyloid peptide antigens define immune response and efficacy in APP transgenic mice. *Proc. Natl. Acad. Sci. U. S. A.* *104*, 9810–5.
- (42) Milletti, F. (2012) Cell-penetrating peptides: classes, origin, and current landscape. *Drug Discovery Today* *17*, 850–60.
- (43) Gautam, A., Singh, H., Tyagi, A., Chaudhary, K., Kumar, R., Kapoor, P., and Raghava, G. P. (2012) CPPsite: a curated database of cell penetrating peptides. *Database* *2012*, bas015.
- (44) Lu, W. (2012) Adsorptive-mediated brain delivery systems. *Curr. Pharm. Biotechnol.* *13*, 2340–8.
- (45) Bickel, U., Yoshikawa, T., and Pardridge, W. M. (2001) Delivery of peptides and proteins through the blood–brain barrier. *Adv. Drug Delivery Rev.* *46*, 247–79.
- (46) Lalatsa, A., Schatzlein, A. G., and Uchegbu, I. F. (2014) Strategies to deliver peptide drugs to the brain. *Mol. Pharmaceutics* *11*, 1081–93.
- (47) Banks, W. A., Kastin, A. J., Maness, L. M., Huang, W., and Jaspán, J. B. (1995) Permeability of the blood–brain barrier to amylin. *Life Sci.* *57*, 1993–2001.
- (48) Banks, W. A., Jaspán, J. B., Huang, W., and Kastin, A. J. (1997) Transport of insulin across the blood–brain barrier: saturability at euglycemic doses of insulin. *Peptides* *18*, 1423–9.
- (49) Nonaka, N., Shioda, S., Niehoff, M. L., and Banks, W. A. (2003) Characterization of blood–brain barrier permeability to PYY3–36 in the mouse. *J. Pharmacol. Exp. Ther.* *306*, 948–953.
- (50) Banks, W. A., Goulet, M., Rusche, J. R., Niehoff, M. L., and Boismenu, R. (2002) Differential transport of a secretin analog across

the blood–brain and blood-cerebrospinal fluid barriers of the mouse. *J. Pharmacol. Exp. Ther.* 302, 1062–1069.

(51) Demeule, M., Regina, A., Che, C., Poirier, J., Nguyen, T., Gabathuler, R., Castaigne, J. P., and Beliveau, R. (2008) Identification and design of peptides as a new drug delivery system for the brain. *J. Pharmacol. Exp. Ther.* 324, 1064–1072.

(52) Sarkar, G., Curran, G. L., Mahlum, E., Decklever, T., Wengenack, T. M., Blahnik, A., Hoesley, B., Lowe, V. J., Poduslo, J. F., and Jenkins, R. B. (2011) A carrier for non-covalent delivery of functional beta-galactosidase and antibodies against amyloid plaques and IgM to the brain. *PLoS One* 6, e28881.

(53) Côrte-Real, S., Neves, V., Oliveira, S., Canhão, P., Outeiro, T., Castanho, M., and Aires da Silva, F. Antibody Molecules And Peptide Delivery Systems For Use In Alzheimer's Disease And Related Disorders. WO2016/120843 A1, 2016.

(54) Neves, V., Aires-da-Silva, F., Corte-Real, S., and Castanho, M. A. R. B. (2016) Antibody Approaches To Treat Brain Diseases. *Trends Biotechnol.* 34, 36.

(55) Farrington, G. K., and Sisk, W. Enhancement of transport of therapeutic molecules across the blood brain barrier. WO/2013/106577, 2013.

(56) Morais, M., Oliveira, B. L., Correia, J. D., Oliveira, M. C., Jimenez, M. A., Santos, I., and Raposinho, P. D. (2013) Influence of the bifunctional chelator on the pharmacokinetic properties of  $^{99m}\text{Tc}$ -(CO)<sub>3</sub>-labeled cyclic alpha-melanocyte stimulating hormone analog. *J. Med. Chem.* 56, 1961–73.

(57) Scasnar, V., and van Lier, J. E. (1993) The use of SEP-PAK SI cartridges for the preparation of gallium chloride from the citrate solution. *Eur. J. Nucl. Med.* 20, 273.

(58) Alves, S., Correia, J. D., Gano, L., Rold, T. L., Prasanphanich, A., Haubner, R., Rupprich, M., Alberto, R., Decristoforo, C., Santos, I., and Smith, C. J. (2007) In vitro and in vivo evaluation of a novel  $^{99m}\text{Tc}$ -(CO)<sub>3</sub>-pyrazolyl conjugate of cyclo-(Arg-Gly-Asp-d-Tyr-Lys). *Bioconjugate Chem.* 18, 530–7.

(59) Li, G., Simon, M. J., Cancel, L. M., Shi, Z. D., Ji, X., Tarbell, J. M., Morrison, B., 3rd, and Fu, B. M. (2010) Permeability of endothelial and astrocyte cocultures: in vitro blood–brain barrier models for drug delivery studies. *Ann. Biomed. Eng.* 38, 2499–511.